[CANCER RESEARCH 61, 5106–5115, July 1, 2001]

Pharmacological Inhibitors of the Mitogen-activated Protein Kinase (MAPK) Kinase/MAPK Cascade Interact Synergistically with UCN-01 to Induce Mitochondrial Dysfunction and Apoptosis in Human Leukemia Cells[1]

Yun Dai, Chunrong Yu, Victor Singh, Lin Tang, Zhiliang Wang, Robert McInistry, Paul Dent, and Steven Grant[2]

Division of Hematology/Oncology [Y. D., C. Y., V. S., Z. W., S. G.], Departments of Pharmacology [S. G.], Biochemistry [S. G.], Microbiology [L. T., S. G.], and Radiation Oncology [R. M., P. D.], Medical College of Virginia, Richmond, Virginia 23298

ABSTRACT

Interactions between the checkpoint abrogator UCN-01 and several pharmacological inhibitors of the mitogen-activated protein kinase (MAPK) kinase (MEK)/MAPK pathway have been examined in a variety of human leukemia cell lines. Exposure of U937 monocytic leukemia cells to a marginally toxic concentration of UCN-01 (*e.g.*, 150 nM) for 18 h resulted in phosphorylation/activation of p42/44 MAPK. Coadministration of the MEK inhibitor PD184352 (10 μM) blocked UCN-01-induced MAPK activation and was accompanied by marked mitochondrial damage (*e.g.*, cytochrome *c* release and loss of $\Delta\Psi_m$), caspase activation, DNA fragmentation, and apoptosis. Similar interactions were noted in the case of other MEK inhibitors (*e.g.*, PD98059; U0126) as well as in multiple other leukemia cell types (*e.g.*, HL-60, Jurkat, CCRF-CEM, and Raji). Coadministration of PD184352 and UCN-01 resulted in reduced binding of the cdc25C phosphatase to 14-3-3 proteins, enhanced dephosphorylation/activation of $p34^{cdc2}$, and diminished phosphorylation of cyclic AMP-responsive element binding protein. The ability of UCN-01, when combined with PD184352, to antagonize cdc25C/14-3-3 protein binding, promote dephosphorylation of $p34^{cdc2}$, and potentiate apoptosis was mimicked by the ataxia telangectasia mutation inhibitor caffeine. In contrast, cotreatment of cells with UCN-01 and PD184352 did not substantially increase c-Jun-NH_2-terminal kinase activation nor did it alter expression of Bcl-2, Bcl-x_L, Bax, or X-inhibitor of apoptosis. However, coexposure of U937 cells to UCN-01 and PD184352 induced a marked increase in p38 MAPK activation. Moreover, SB203580, which inhibits multiple kinases including p38 MAPK, partially antagonized cell death. Lastly, although UCN-01 ± PD184352 did not induce $p21^{CIP1}$, stable expression of a $p21^{CIP1}$ antisense construct significantly increased susceptibility to this drug combination. Together, these findings indicate that exposure of leukemic cells to UCN-01 leads to activation of the MAPK cascade and that interruption of this process by MEK inhibition triggers perturbations in several signaling and cell cycle regulatory pathways that culminate in mitochondrial injury, caspase activation, and apoptosis. They also raise the possibility that disrupting multiple signaling pathways, *e.g.*, by combining UCN-01 with MEK inhibitors, may represent a novel antileukemic strategy.

INTRODUCTION

UCN-01 (7-hydroxystaurosporine) is a derivative of staurosporine that was originally developed as an inhibitor of PKC[3] (1). However, UCN-01 has since been shown to inhibit other kinases, including Chk1, which is responsible for phosphorylation, binding to 14-3-3 proteins, and subsequent degradation of the cdc25c phosphatase (2). Degradation of cdc25c results in phosphorylation and inactivation of CDKs such as CDK1 ($p34^{cdc2}$), which are critically involved in cell cycle arrest after DNA damage and other insults (3). In this way, UCN-01 acts as a checkpoint abrogator, an action that may account for its ability to enhance the lethal actions of various cytotoxic agents, including cisplatin (4), mitomycin C (5), camptothecin (6), fludarabine (7), gemcitabine (8), and 1-β-D-arabinofuranosylcytosine (9, 10), among others. When administered alone, UCN-01 induces arrest in G_2M or G_0G_1, depending upon cell type, or, alternatively, the p53 or pRb status of the cell (11, 12). UCN-01 is also a potent inducer of apoptosis, particularly in hematopoietic cells, a phenomenon that appears to be more closely related to dephosphorylation of CDKs than to inhibition of PKC (13).

Phase I and pharmacokinetic studies of UCN-01 have been initiated in humans and have shown that this compound exhibits a very long plasma half-life, presumably a consequence of extensive binding to α_1 acidic glycoprotein (14). Nevertheless, free plasma levels of UCN-01 capable of inhibiting Chk 1 and abrogating checkpoint control events appear to be achievable (15, 16). In a preliminary study (16), combination of UCN-01 with established cytotoxic agents was associated with evidence of clinical activity in a patient with advanced non-Hodgkin's lymphoma, raising the possibility that UCN-01 may enhance the *in vivo* activity of conventional chemotherapeutic drugs.

Despite the intense interest in UCN-01 as an antineoplastic agent, the mechanism(s) by which it induces cell death remain(s) incompletely understood. Recently, considerable attention has focused on the role of signal transduction pathways in the regulation of cell survival, particularly those related to three parallel MAPK modules. Of these, the SAPK/JNK and p38 kinase are primarily induced by environmental insults (*e.g.*, DNA damage or osmotic stress) and are generally associated with pro-apoptotic actions (17, 18). In contrast, p42/44 MAPKs (ERKs) are induced by mitogenic or differentiation-related stimuli and are most frequently (although not invariably) associated with pro-survival activity (19, 20). In fact, there is evidence that the relative outputs of the JNK and p42/44 MAPK cascades determine whether a cell lives or dies in response to a noxious stimulus (*e.g.*, growth factor deprivation; Ref. 21). p42/44 MAPK lies downstream of a signaling pathway consisting of PKC, Raf-1, and MEK1 (22). Investigation of the functional role of p42/44 MAPK in cell death decisions, as well as other biological processes, has been greatly facilitated by the development of pharmacological MEK inhibitors, including PD98059 (23), U0126 (24), and SL327 (25). Recently, Seybolt-Leopold *et al.* (26) described a novel MEK inhibitor, PD184352, which is able to block MAPK activation and to inhibit the *in vivo* growth of colon tumor cells in mice. Aside from their intrinsic antitumor activity, MEK inhibitors may also have a role as potentiators of established chemotherapeutic drug action (27).

The relationship between UCN-01 actions and activity of the

Received 1/10/01; accepted 4/20/01.

The costs of publication of this article were defrayed in part by the payment of page charges. This article must therefore be hereby marked *advertisement* in accordance with 18 U.S.C. Section 1734 solely to indicate this fact.

[1] Supported by Awards CA 63753, CA 77141, and DK 52825 from the NIH, and by Awards 6630-01 from the Leukemia and Lymphoma Society of America and BC980148 from the Department of Defense.

[2] To whom requests for reprints should be addressed, at Division of Hematology/Oncology, Medical College of Virginia, MCV Station Box 230, Richmond, VA 23298. Phone: (804) 828-5211; Fax: (804) 828-8079; E-mail: stgrant@hsc.vcu.edu.

[3] The abbreviations used are: PKC, protein kinase C; CDK, cyclin-dependent kinase; MAPK, mitogen-activated protein kinase; MEK, MAPK kinase; SAPK, stress-activated protein kinase; JNK, c-Jun NH_2-terminal kinase; ERK, extracellular regulated kinase; TUNEL, terminal deoxynucleotidyl transferase-mediated nick end labeling; $DiOC_6$, 3,3-dihexyloxacarbocynine; BrdUrd, bromodeoxyuridine; CREB, cyclic AMP-responsive element binding protein; PARP, poly(ADP-ribose) polymerase; RIPA, radioimmunoprecipitation assay; CHX, cycloheximide; GFX, bisindolylmaleimide; PMA, phorbol 12-myristate 13-acetate.

MAPK pathway is poorly understood. Given the fact that UCN-01 can function as a PKC inhibitor (1) and that it has been shown to mimic some of the actions of the PKC down-regulator bryostatin 1 as well as the kinase inhibitor staurosporine (25), the possibility that UCN-01 might block the downstream PKC targets MEK1/2 and MAPK appeared plausible. To address this issue, we have examined the apoptotic actions of UCN-01 in relation to its effects on the MEK/MAPK cascade. Contrary to expectations, exposure of multiple myeloid and lymphoid cell lines to submicromolar concentrations of UCN-01 potentiated, rather than reduced, MAPK phosphorylation/activation. Moreover, interference with this process by several pharmacological MEK inhibitors, including PD98059, U0126, and PD184352, resulted in a highly synergistic enhancement of mitochondrial damage, caspase activation, and apoptosis in these cells. Together, these findings suggest that exposure of human leukemia cells to UCN-01 elicits a cytoprotective MAPK response and raise the possibility that combining this agent with pharmacological MEK inhibitors may effectively lower the apoptotic threshold.

MATERIALS AND METHODS

Cells. U937, HL-60, Jurkat, CCRF-CEM, and Raji cells are human histiocytic lymphoma, acute promyelocytic leukemia, acute T-cell leukemia, acute lymphoblastic leukemia, and Burkitt lymphoma cell lines, respectively. All of the cells were derived by the American Type Culture Collection and maintained in RPMI 1640 medium containing 10% FBS, 200 units/ml penicillin, 200 μg/ml streptomycin, minimal essential vitamins, sodium pyruvate, and glutamine, as reported previously (28). U937/p21AS and U937/pREP4 cells were obtained by stable transfection of cells with plasmids containing antisense-oriented p21 cDNA or an empty vector (pREP4), and clones were selected with hygromycin (29).

Drugs and Reagents. Selective MEK inhibitors (PD98059 and UO126), selective PKC inhibitors (GF 109203X or GFX I and safingol), and specific inhibitors of p38 MAPK (SB203580) were supplied by Calbiochem (San Diego, CA) as powder. The MEK inhibitor PD184352 was kindly provided by Dr. Judith Sebolt-Leopold (Warner Lambert/Parke-Davis Co., Ann Arbor, MI). Materials were dissolved in sterile DMSO and stored frozen under light-protected conditions at −20°C. UCN-01 was kindly provided by Dr. Edward Sausville (Developmental Therapeutics Program/Cancer Treatment and Evaluation Program (CTEP), National Cancer Institute). It was dissolved in DMSO at a stock concentration of 1 mM, stored at −20°C, and subsequently diluted with serum-free RPMI medium before use. Caffeine (Alexis Co., San Diego, CA) was dissolved in chloroform and stored at −20°C. In all of the experiments, the final concentration of DMSO or chloroform did not exceed 0.1%. Caspase inhibitor (Z-VAD-fmk) and caspase 8 inhibitor (Z-IETD-fmk) were purchased from Enzyme System Products (Livermore, CA), dissolved in DMSO, and stored at 4°C. Cycloheximide was purchased from Sigma Chemical Co. (St. Louis, MO), stored frozen in DMSO, and diluted in RPMI 1640 medium before use.

Experimental Format. All of the experiments were performed using logarithmically growing cells (3–5 $\times$ 10^5 cells/ml). Cell suspensions were placed in sterile 25 cm^2 T-flasks (Corning, Corning, NY) and incubated with MEK or PKC inhibitors for 30 min at 37°C. At the end of this period, UCN-01 (or in some cases, caffeine) was added to the suspension, and the flasks were placed in 37°C/5% CO_2 incubator at various intervals, generally 18 h. In some studies, the p38 MAP kinase inhibitor SB203580 was added concurrently with MEK inhibitors. After drug treatment, cells were harvested and subjected to further analysis as described below.

Analysis of Apoptosis. The extent of apoptosis was evaluated by assessment of Wright-Giemsa-stained preparation under light microscopy and scoring the number of cells exhibiting classic morphological features of apoptosis. For each condition, 5 to 10 randomly selected fields/condition were evaluated, encompassing at least 500 cells (28). To confirm the results of morphological analysis, in some cases cells were also evaluated by TUNEL staining (30) and assessment of oligonucleosomal DNA fragmentation of total DNA. DNA fragmentation was analyzed by 1.8% agarose gel electrophoresis as described previously (31). For TUNEL staining, cytocentrifuge preparations were obtained and fixed with 4% formaldehyde. The slides were treated with acetic acid/ethanol (1:2), stained with terminal transferase reaction mixture containing 1 $\times$ terminal transferase reaction buffer, 0.25 units/μl terminal transferase, 2.5 mM $CoCl_2$, and 2 pmol fluorescein-12-dUTP (Boehringer Mannheim, Indianapolis, IN), and visualized using fluorescence microscopy.

Analysis of Mitochondrial Membrane Potential ($\Delta\Psi$m). Cells (2 $\times$ 10^5) were incubated with 40 nM $DiOC_6$ (Molecular Probes Inc., Eugene, OR) in PBS at 37°C for 20 min and then analyzed by flow cytometry as described previously (29). The percentage of cells exhibiting a low level of $DiOC_6$ uptake, which reflects loss of mitochondrial membrane potential, was determined using a Becton Dickinson FACScan (Becton Dickinson, San Jose, CA).

Cell Cycle Analysis and S-phase Content. Cells (2 $\times$ 10^6) were pelleted at 4°C, resuspended, fixed at 4°C with 67% ethanol overnight, and treated on ice with a propidium iodide solution containing 3.8 mM Na citrate, 0.5 mg/ml RNase A (Sigma Chemical Co.), and 0.01 mg/ml propidium iodide (Sigma Chemical Co.) for 3 h. Cell cycle analysis was performed by flow cytometry using Verity Winlist software (Topsham, ME).

Incorporation of BrdUrd was monitored to evaluate S-phase content. For each condition, 2 $\times$ 10^6 cells (cell density = 5 $\times$ 10^5/ml) were incubated with 10 μM BrdUrd for 30 min at 37°C. After washing twice with 1% BSA/PBS, the cells were resuspended in 70% ethanol and fixed for 30 min on ice. The BrdUrd-labeled cells were denatured and nuclei released by incubation with 2 N HCl/0.5% Triton X-100 for 30 min at room temperature. After centrifugation, the pellet was resuspended in 0.1 M $Na_2B_4O_4$ (pH 8.5) to neutralize the acid. Cells (1×10^6)/100 μl in 0.5% Tween 20/1% BSA/PBS were incubated with FITC-conjugated anti-BrdUrd (1:10; mouse monoclonal; DAKO, Carpinteria, CA) for 30 min at 4°C. After washing once with 0.5% Tween 20/1% BSA/PBS, the cells were resuspended in PBS containing 5 μg/ml propidium iodide and analyzed by flow cytometry. The percentage of S-phase cells was determined by measuring BrdUrd FITC-positive part in a dot plot of FL-3 (red fluorescence) against FL-1 (green fluorescence).

Immunoblot and Immunoprecipitation Analysis. Whole-cell pellets were lysed by sonication in 1 $\times$ sample buffer [62.5 mM Tris base (pH6.8), 2% SDS, 50 mM DTT, 10% glycerol, 0.1% bromphenol blue, and 5 μg/ml each chymostatin, leupeptin, aprotinin, pepstatin, and soybean trypsin inhibitor] and boiled for 5 min. For analysis of phospho-proteins, 1 mM each Na vanadate and Na PP_i was added to the sample buffer. Protein samples were collected from the supernatant after centrifugation of the samples at 12,800 $\times$ g for 5 min, and protein was quantified using Coomassie Protein Assay Reagent (Pierce, Rockford, IL). Equal amounts of protein (30 μg) were separated by SDS-PAGE and electrotransferred onto a nitrocellulose membrane. For blotting phosphoproteins, no SDS was included in the transfer buffer. The blots were blocked with 5% milk in PBS-Tween 20 (0.1%) at room temperature for 1 h and probed with the appropriate dilution of primary antibody overnight at 4°C. The blots were washed twice in PBS-Tween 20 for 15 min and then incubated with a 1:2000 dilution of horseradish peroxidase-conjugated secondary antibody (Kirkegaard & Perry, Gaithersburg, MD) in 5% milk/PBS-Tween 20 at room temperature for 1 h. After washing twice in PBS-Tween 20 for 15 min, the proteins were visualized by Western Blot Chemiluminescence Reagent (NEN Life Science Products, Boston, MA). For analysis of phospho-proteins, Tris-buffered saline was used instead of PBS throughout. Where indicated, the blots were reprobed with antibodies against actin (Signal Transduction Laboratories) or tubulin (Calbiochem) to ensure equal loading and transfer of proteins. The following antibodies were used as primary antibodies: phospho-p44/42 MAPK (Thr202/Tyr204) antibody (1:1000; rabbit polyclonal; NEB, Beverly, MA); p44/42 MAPK antibody (1:1000; rabbit polyclonal; NEB); phospho-p38 MAPK (Thr180/Tyr182) antibody (1:1000; rabbit polyclonal; NEB); phospho-SAPK/JNK (Thr183/Tyr185) antibody (1:1000; rabbit polyclonal; Cell Signaling Technology, Beverly, MA); SAPK/JNK antibody (1:1000; rabbit polyclonal; Cell Signaling Technology); anti-phospho-CREB (1:1000; rabbit polyclonal; Upstate Biotechnology, Lake Placid, NY); phospho-cdc2 (Tyr15) antibody (1:1000; rabbit polyclonal; Cell Signaling Technology); anti-p21Cip/WAF1 (1:500; mouse monoclonal; Transduction Laboratories, Lexington, KY); anti-p27kip1 (1:500; mouse monoclonal; PharMingen, San Diego, CA); MAP kinase phosphatase-1 (M-18; 1:200; rabbit polyclonal; Santa Cruz Biotechnology Inc., Santa Cruz, CA); MAP kinase phosphatase-3 (C-20; 1:100; goat polyclonal; Santa Cruz Biotechnology Inc.); antihuman Bcl-2 oncoprotein (1:2000; mouse monoclonal; DAKO, Carpinteria, CA); Bax (N-20; 1:2000; rabbit polyclonal; Santa Cruz Biotechnology Inc.); Bcl-$x_{S/L}$ (S-18; 1:500;

rabbit polyclonal; Santa Cruz Biotechnology Inc.); antihuman/mouse XIAP (1:500; rabbit polyclonal; R&D System, Minneapolis, MN); anti-caspase-3 (1:1000; rabbit polyclonal; PharMingen); cleaved-caspase-3 (M_r 17,000) antibody (1:1000; rabbit polyclonal; Cell Signaling Technology); anti-caspase-9 (1:1000; rabbit polyclonal; PharMingen); anti-PARP (1:2500; mouse monoclonal; Calbiochem); and cleaved PARP (M_r 89,000) antibody (1:1000; rabbit polyclonal; Cell Signaling Technology).

Immunoprecipitation was performed to determine the extent of cdc25C activation (32). Briefly, 2×10^7 cells were lysed in RIPA buffer (1% NP40, 0.5% Na deoxycholate, 1 mM phenylmethylsulfonyl fluoride, 1 mM Na vanadate, 5 μg/ml chymostatin, leupeptin, aprotinin, pepstatin, and soybean trypsin inhibitor, and 0.1% SDS in PBS) by syringing approximately 20 times with a 23-gauge needle. Protein samples were centrifuged at 12,800 $\times$ *g* for 30 min and quantified. Two-hundred μg of protein/condition were incubated under continuous shaking with 1 μg of anti-cdc25C (mouse monoclonal; PharMingen) overnight at 4°C. Twenty μl/condition of Dynabeads (goat antimouse IgG; Dynal, Oslo, Norway) were added and incubated for an additional 4 h. After washing three times with RIPA buffer, the bead-bound protein was eluted by vortexing and boiling in 20 μl of 1 $\times$ sample buffer. The samples were separated by 12% SDS-PAGE and subjected to immunoblot analysis as described above. Anti-14-3-3β (rabbit polyclonal; Santa Cruz Biotechnology Inc.) was used as primary antibody at a dilution of 1:200.

Analysis of Cytosolic Cytochrome *c*. Cells (2×10^6) were washed in PBS and lysed by incubating for 30 s in lysis buffer (75 mM NaCl, 8 mM Na_2HPO4, 1 mM NaH_2PO4, 1 mM EDTA, and 350 μg/ml digitonin). The lysates were centrifuged at 12,000 $\times$ *g* for 1 min, and the supernatant was collected and added to an equal volume of 2 $\times$ sample buffer. The protein samples were quantified, separated by 15% SDS-PAGE, and subjected to immunoblot analysis as described above. Anticytochrome *c* (mouse monoclonal; PharMingen) was used as primary antibody at a dilution of 1:500.

Cdk1/cdc2 Kinase Assay. Cdk1/cdc2 Kinase Assay Kit (Upstate Biotechnology) was used to determine the activity of cdk1/cdc2 kinase according to the manufacturer's instructions. Briefly, 2×10^7 cells were lysed in RIPA buffer by sonication. Protein samples were centrifuged at 12,800 $\times$ *g* for 30 min and quantified. Fifty μg of protein/condition were incubated with 400 μg/ml histone H1, 2 μCi of [γ-^{32}P]ATP, and 1:5 inhibitor cocktail in assay dilution buffer (total volume, 50 μl) at 30°C for 20 min. A 25-μl aliquot of reaction mixture was transferred onto P81 paper. After washing three times with 0.75% phosphoric acid and once with acetone, cpm of [γ-^{32}P] incorporated into histone H1 was monitored using TRI-CARB 2100TR Liquid Scintillation Analyzer (Packard Instrument Co., Downers Grove, IL). In some cases, 10 μl of 2 $\times$ sample buffer was added to 10 μl of the reaction mixture and boiled for 5 min. [γ-^{32}P]histone H1 was separated by 12% SDS-PAGE and visualized by exposure of the dried gels to X-ray film (KODAK) at -80°C for 1 h.

Clonogenic Assay and Cell Proliferation Assays. Colony formation after drug treatment was evaluated using a soft agar cloning assay as described previously (33). Briefly, cells were washed three times with serum-free RPMI medium. Subsequently, 500 cells/well were mixed with RPMI medium containing 20% FBS and 0.3% agar and plated on 12-well plates (three wells/condition). The plates were then transferred to a 37°C/5% CO_2, fully humidified incubator. After 10 days of incubation, colonies, consisting of groups of >50 cells, were scored using an Olympus Model CK inverted microscope, and colony formation for each condition was calculated in relation to values obtained for untreated control cells. For cell viability assays, CellTiter 96 AQueous One Solution (Promega, Madison, WI) was used according to the manufacturer's instructions, and the absorbance at 490 nm was recorded using a 96-well plate reader (Molecular Devices, Sunnyvale, CA).

Normal Peripheral Blood Mononuclear Cells. Peripheral blood was obtained with informed consent from normal volunteers, diluted 1:3 with RPMI 1640 medium, and layered over a cushion of 10 ml of Ficoll-Hypaque (specific gravity, 1.077; Sigma Chemical Co.) in sterile 50-ml plastic centrifuge tubes. These studies have been approved by the Human Investigations Committee of Virginia Commonwealth University. After centrifugation for 40 min at 400 $\times$ *g* at room temperature, the interface layer, consisting of mononuclear cells, was extracted with a sterile Pasteur pipette and diluted in fresh RPMI medium. The cells were washed $\times$2 in medium and resuspended in RPMI 1640 medium containing 10% FCS in 25-cm^2 tissue culture flasks at a cell density of 10^6 cells/ml. Various concentrations of UCN-01 $\pm$ PD 184352 were added to the flasks, after which they were placed in the incubator for 24 h. At the end of this period, cytospin preparations were obtained and stained with Wright-Giemsa, and the cells were scored under light microscopy for the typical morphological features of apoptosis.

Statistical Analysis. For morphological assessment of apoptotic cells, cell cycle analysis, S-phase content, cdk1/cdc2 kinase assay, analysis of $\Delta\Psi$m, and clonogenic and cell proliferation assays, experiments were repeated at least three times. Values represent the means $\pm$ SD for at least three separate experiments performed in triplicate. The significance of differences between experimental variables was determined using the Student *t* test.

RESULTS

The effects of combined exposure of human monocytic leukemia cells (U937) to UCN-01 and the MEK inhibitor PD184352 were first examined in relation to MAPK activation and apoptosis (Fig. 1). Unexpectedly, incubation with UCN-01 (150 nM) induced phosphorylation (activation) of MAPK by 2 h, and this effect persisted over the ensuing 18 h (Fig. 1*A*). Coincubation of U937 cells with PD184532 (10 μM) attenuated induction of phospho-MAPK at 2 h, and inhibition of MAPK activation was essentially complete after 18 h. To determine what impact this phenomenon had on cell fate, the extent of apoptosis was monitored in cells exposed to each agent individually and in combination. Whereas exposure to PD184352 or

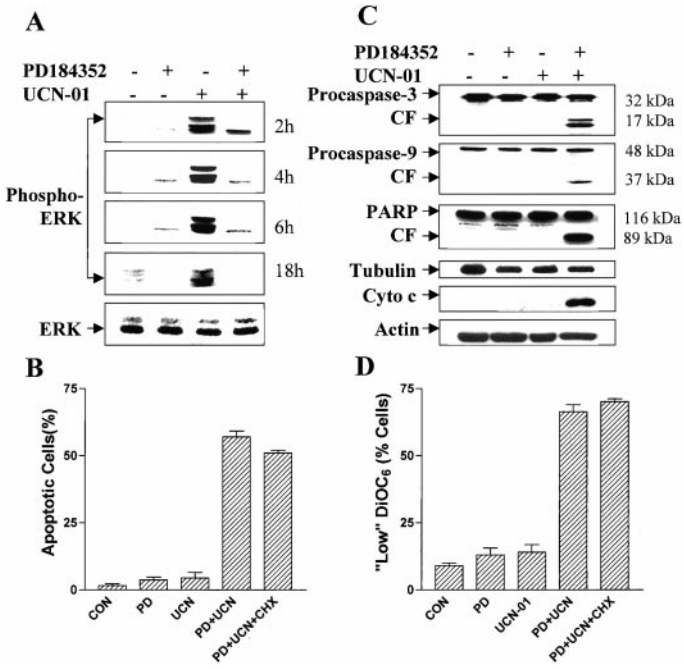

Fig. 1. *A*, logarithmically growing U937 cells were incubated for the designated intervals in the presence of 150 nM UCN-01 $\pm$ 10 μM PD184352, after which cells were lysed, and proteins were separated by SDS-PAGE and probed with antibodies directed against phospho-ERK, as described in "Materials and Methods." Blots were subsequently stripped and reprobed with antibodies directed against total ERK. Two additional studies yielded equivalent results. *B*, cells were treated with PD184352 (*PD*) and/or UCN-01 (*UCN*; $\pm$1 μM CHX) as above for 18 h, after which Wright Giemsa-stained cytospin preparations were evaluated by light microscopy, and the percentage of cells exhibiting classic apoptotic features was determined by examining 5–10 randomly selected fields encompassing $\geq$500 cells. Values represent the means $\pm$ SD for three separate experiments performed in triplicate. *C*, cells were treated as in *A*, and the proteins were separated by SDS-PAGE and probed with antibodies directed against caspase-3, caspase-9, or PARP. *CF*, cleavage fragment. Alternatively, cytosolic fractions were obtained as described in "Materials and Methods," and expression of cytochrome *c* was monitored as above. Each *lane* was loaded with 30 μg of protein. Blots were stripped and reprobed with antibodies to actin or tubulin to ensure equal loading and transfer. *D*, cells were treated with UCN-01 $\pm$ PD184352 ($\pm$ 1 μM cycloheximide) as above, after which the percentage of cells exhibiting reduced mitochondrial membrane potential ($\Delta\Psi_m$) was determined by monitoring $DiOC_6$ uptake as described in "Materials and Methods." Results represent the means $\pm$ SD for three separate experiments performed in triplicate.

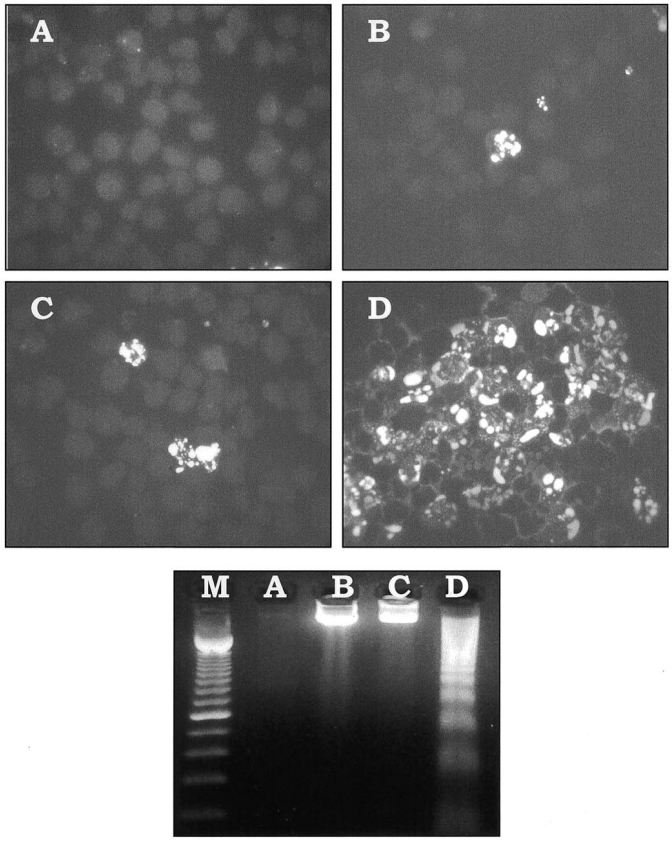

Fig. 2. *Top panels*, cells were exposed to UCN-01 (150 nM) ± PD184352 (10 μM) as above for 18 h, after which cytospin preparations were obtained and TUNEL staining was performed as described in "Materials and Methods." Cells were then viewed under fluorescence microscopy at ×50 magnification. *A*, control; *B*, PD1843252; *C*, UCN-01; *D*, UCN-01 + PD184352. *Bottom panel*, cells were treated as above after which cells were lysed, and DNA was extracted, separated by agarose gel electrophoresis, and stained with ethidium bromide as described in "Materials and Methods." *Lanes* (20 μg of DNA each): *M*, molecular weight marker; *A*, control; *B*, PD184352; *C*, UCN-01; *D*, UCN-01 + PD184352.

150 nM UCN-01 alone was minimally toxic to these cells (<10% apoptosis in each case), combined treatment resulted in a dramatic increase in cell death (*i.e.*, ~60%; Fig. 1*B*). Furthermore, this effect was not attenuated by coadministration of the protein synthesis inhibitor CHX (1 μM). Consistent with these findings, combined treatment with UCN-01 and PD184352, but not individual exposure, induced marked cleavage of procaspases-3 and -9, PARP degradation, and cytochrome *c* release into the cytoplasmic S-100 fraction (Fig. 1*C*). Cotreatment of cells with UCN-01 and PD184352 also resulted in a marked increase in the number of cells exhibiting loss of the mitochondrial membrane potential (*e.g.*, $\Delta\psi_m$; Fig. 1*D*), an action that was also not attenuated by CHX. TUNEL assays confirmed that a small number of cells exposed to UCN-01 or PD184352 alone for 18 h (Fig. 2, *B* and *C*) displayed DNA breaks containing overhanging 3′-OH ends, whereas coexposure resulted in a high percentage of TUNEL-positive cells. Similarly, agarose gel electrophoresis demonstrated a marked increase in oligonucleosomal DNA fragmentation in cells exposed to both agents (Fig. 2; *bottom panel*). Together, these findings indicate that coadministration of the MEK inhibitor PD184352 blocks MAPK activation and dramatically increases apoptosis in U937 cells exposed to a marginally toxic concentration of UCN-01.

To determine whether these findings could be extended to other known MEK inhibitors, U937 cells were incubated for 24 h with 200 nM UCN-01 either alone or in combination with PD98059 (50 μM), an aminoflavone that was among the earliest of the MEK inhibitors to be investigated (23), and U0126 (20 μM), the affinity of which for the CDK ATP-binding site is significantly greater than that of PD98059 (24). As noted in the case of PD184352, coadministration of minimally toxic concentrations of PD98059 or U0126 with 200 nM UCN-01 resulted in a marked potentiation of cell death, manifested by an increase in the morphological features of apoptosis (Fig. 3, *A* and *C*), PARP degradation, and release of cytochrome *c* into the cytoplasm (Fig. 3, *B* and *D*). These findings demonstrated that multiple pharmacological MEK inhibitors are capable of substantially increasing the lethal actions of UCN-01 toward U937 cells.

To establish whether the enhanced lethality of MEK inhibitors and UCN-01 was restricted to U937 cells or, instead, might be generalized to include other leukemia cell types, the effects of combined exposure to UCN-01 and PD184352 were examined in several additional leukemia cell lines (Fig. 4). Because the sensitivity of these cells to UCN-01 differed somewhat from that of U937 cells, slightly higher UCN-01 concentrations (*e.g.*, 150–300 nM) were used in some cases. On the basis of standard morphological criteria as well as evidence of PARP degradation, it can be seen that combined treatment with UCN-01 and PD184352, administered at concentrations that were marginally toxic by themselves, resulted in a dramatic increase in cell death in HL-60 promyelocytic leukemia cells, T-lymphoblastic CCRF-CEM and Jurkat cells, and B-lymphoblastic lymphoma Raji cells (Fig. 4, *A* and *B*). Qualitatively similar results were obtained when PD98059 and U0126 were used (data not shown). As in the case of U937 cells, UCN-01 treatment resulted in a substantial increase in MAPK activation in HL-60, CCRF-CEM, and in Jurkat cells (Fig. 4*C*); moreover, this effect was blocked by PD184352 (5 μM). Thus, combined treatment with UCN-01 and MEK inhibitors prevented MAPK activation and produced a dramatic increase in apoptosis in a variety of myeloid and lymphoid cell lines.

To investigate the hierarchy of events accompanying apoptosis induced by these agents, U937 cells were exposed to the combination of UCN-01 (150 nM) in conjunction with 10 μM PD184352 in the

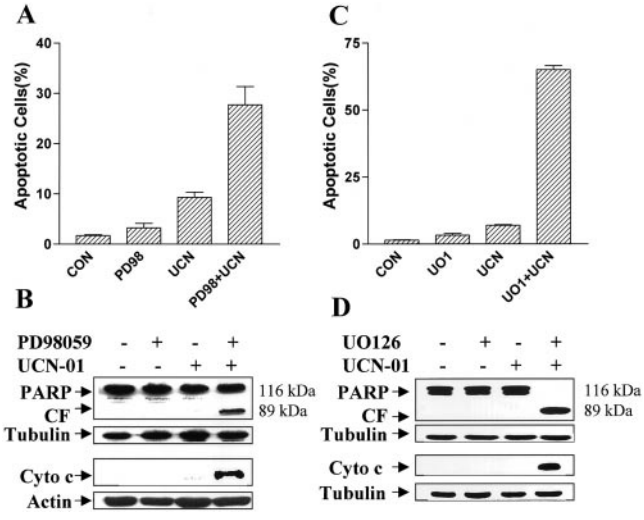

Fig. 3. *A*, U937 cells were exposed to UCN-01 (200 nM; *UCN*) ± PD98059 (50 μM; *PD98*) for 24 h, after which the percentage of apoptotic cells was scored as described above (Fig. 1). *B*, cells were exposed to UCN-01 (200 nM) ± PD98059 (50 μM) for 24 h, after which cells were lysed, and proteins were separated by SDS-PAGE and probed for expression of PARP and cytosolic cytochrome *c* as described in Fig. 1. *CF*, cleavage fragment. *C*, cells were exposed to UCN-01 (200 nM) ± 20 μM U0126 (*UO1*) for 24 h, after which apoptosis was determined as in *A*. *D*, cells were exposed to UCN-01 ± U0126 as above, after which expression of PARP and cytosolic cytochrome *c* were determined as above. For *A* and *C*, values represent the means ± SD for three separate experiments performed in triplicate. For *B* and *D*, each *lane* was loaded with 30 μg of protein. Blots were stripped and reprobed with antibodies directed against actin or tubulin to ensure equal loading and transfer. Two additional studies yielded equivalent results.

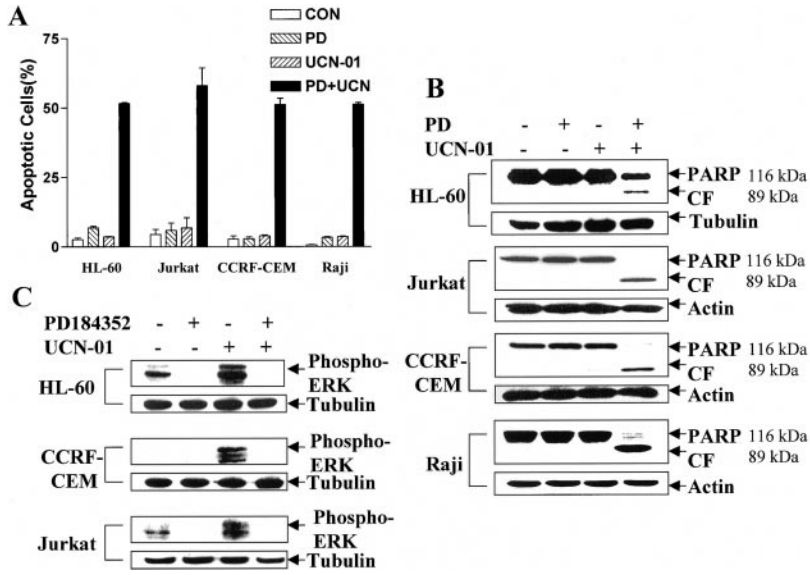

Fig. 4. *A*, HL-60 promyelocytic leukemia cells, Jurkat and CCRF-CEM lymphoblastic leukemia cells, and Raji B-lymphoblastic leukemia cells were exposed to PD184352 (*PD*; 5 μM) ± UCN-01 (*UCN*; 300 nM HL-60; 150 nM Jurkat; 200 nM CCRF; 200 nM Raji) for 24 h, after which the percentage of apoptotic cells was determined as described above. Values represent the means ± SD for three separate experiments performed in triplicate. *B*, cells were treated as above, after which cells were lysed, and the lysates were separated by SDS-PAGE and probed with antibodies directed against PARP. Each *lane* was loaded with 30 μg of protein. Blots were subsequently stripped and reprobed with antibodies to tubulin or actin to ensure equivalent loading and transfer. *CF*, cleavage fragment. *C*, cells were treated as above, after which Western analysis was performed to assess expression of phospho-ERK as described in "Materials and Methods." For *B* and *C*, the results of a representative experiment are shown; two other studies yielded comparable results.

presence or absence of the broad caspase inhibitor ZVAD-fmk as well as the caspase-8 inhibitor IETD-fmk, after which cytochrome *c* release, loss of $\Delta\psi_m$, caspase activation, PARP degradation, and apoptosis were monitored (Fig. 5). Whereas ZVAD-fmk blocked induction of apoptosis and loss of $\Delta\psi_m$ in U937 cells exposed to UCN-01 and PD 184352, IETD was ineffective (Fig. 5, *A* and *B*). Similarly, ZVAD, but not IETD (20 μM each), prevented procaspase-3 cleavage and PARP degradation (Fig. 5*C*). In contrast, ZVAD, like IETD, failed to reduce cytochrome *c* release in UCN-01/PD184352-treated cells. These findings are compatible with the notion that cytochrome *c* release represents the primary event in UCN-01/PD184352-induced apoptosis, whereas the loss of mitochondrial membrane potential is a secondary process that stems from caspase activation. They also

Table 1 *Effects of combining PD184352 with the PKC inhibitors GFX or safingol on apoptosis and loss of $\Delta\Psi_m$ in U937 cells*

Logarithmically growing U937 cells were exposed to PD184352 (10 μM) ± safingol (2 μM) or GFX (1 μM) for 18 h, after which the percentage of morphologically apoptotic cells or the fraction of cells displaying reduced uptake of $DiOC_6$ was determined as described previously. Values represent the means ± SD for three separate experiments performed in triplicate.

	Apoptotic cells (%)	"Low" $DiOC_6$ (% cells)
Control	1.5 ± 0.3	11.7 ± 1.3
GFX (1 μM)	1.9 ± 0.2	13.2 ± 0.6
PD184352 (10 μM)	2.1 ± 0.1	14.7 ± 1.0
GFX + PD	2.2 ± 0.2	15.7 ± 1.7
Control	1.5 ± 0.2	10.5 ± 0.2
Safingol (2 μM)	1.9 ± 0.2	13.6 ± 0.8
PD184352 (10 μM)	1.8 ± 0.1	12.1 ± 0.2
Safingol + PD	2.4 ± 0.1	16.4 ± 1.1

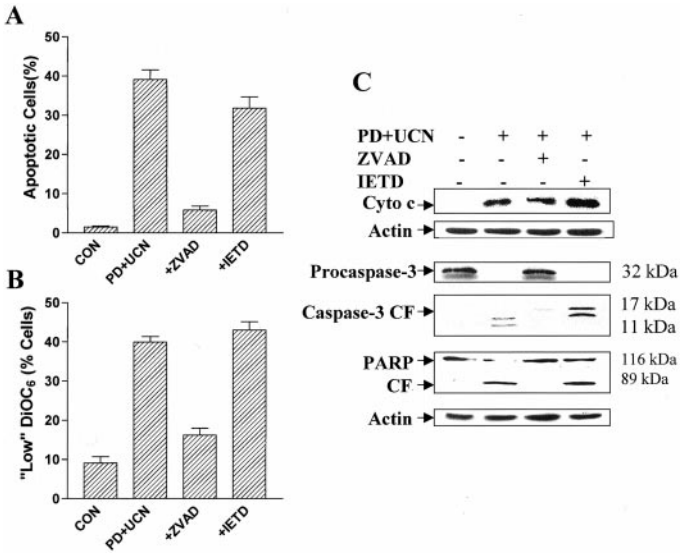

Fig. 5. U937 cells were exposed to PD184352 (*PD*; 10 μM) + UCN-01 (*UCN*; 150 nM) for 10 h in the presence or absence of the broad caspase inhibitor ZVAD-fmk (20 μM) or the caspase-8 inhibitor IETD-fmk (20 μM). At the end of this period, cytospin preparations were monitored for apoptosis by morphological examination of Wright Giemsa-stained specimens (*A*) or the percentage of cells displaying a reduction in $\Delta\Psi_m$ (*B*) determined by flow cytometry as described in "Materials and Methods." Values represent the means ± SD for three separate experiments performed in triplicate. Cells were treated as above, after which protein lysates were subjected to Western analysis to monitor cleavage of full-length procaspase-3 (M_r 32,000) and PARP degradation. *CF*, cleavage fragment. Each *lane* was loaded with 30 μg of protein; an additional study yielded equivalent results.

indicate that UCN-01/PD-induced apoptosis proceeds through a caspase 8-independent pathway.

Because UCN-01 can act as an inhibitor of PKC (1), attempts were made to determine whether this action might be responsible for or contribute to pro-apoptotic interactions with UCN-01. To this end, U937 cells were exposed for 18 h to 10 μM PD 184352 alone or in combination with two known PKC inhibitors, *i.e.*, GFX (1 μM) or safingol (2 μM; Table 1). In separate studies, these drug concentrations were found to block PMA-mediated MAPK phosphorylation in U937 cells (data not shown). In marked contrast to interactions with UCN-01, coadministration of PD 184352 with either GFX or safingol produced relatively minor or no changes in apoptosis or loss of $\Delta\psi_m$, arguing against the possibility that synergism between MEK inhibitors and UCN-01 solely involves PKC inhibition.

Interactions between PD184352 and UCN-01 were then examined in relation to cell cycle events (Fig. 6). Administration of PD184352 by itself for 18 h had little effect on the cell cycle distribution of U937 cells, whereas UCN-01 (150 nM) primarily depleted the G_2M population (Fig. 6*A*). When the agents were combined, elimination of the G_2M fraction persisted, an event accompanied by a significant decline in the S-phase population and corresponding increase in the subdiploid apoptotic fraction. Examination of BrdUrd incorporation, reflecting DNA synthesis, at 12 and 18 h of drug exposure revealed a modest decline in the number of BrdUrd-positive cells after PD184352 treatment, but no effect after incubation with UCN-01 (Fig. 6*B*). However, a very substantial decline in BrdUrd-positive cells was noted 12 h and

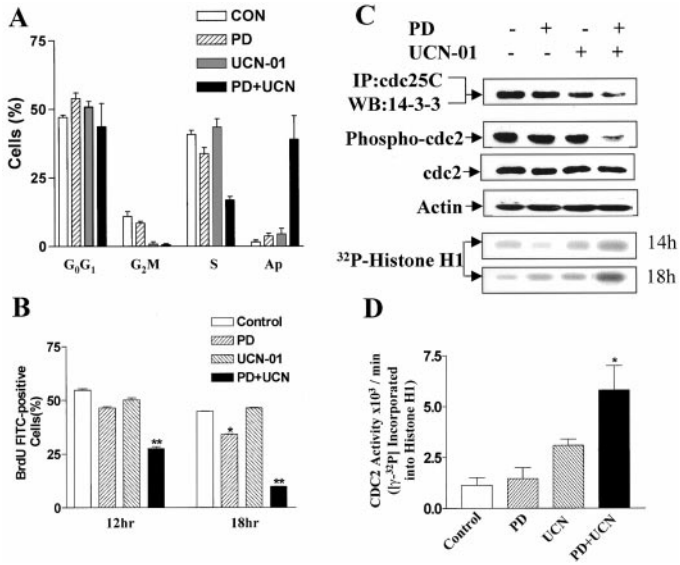

Fig. 6. *A*, U937 cells were exposed to UCN-01 (*UCN*; 150 nM) ± PD1984352 (*PD*; 10 μM) for 12 h and/or 18 h, after which the percentage of cells in G_0G_1, G_2M, S-phase, or the subdiploid fraction (*Ap*) was determined as described in "Materials and Methods." *B*, alternatively, cells were exposed to the same agents for 12 h or 18 h, after which the percentage of BrdUrd FITC-positive (S-phase) cells was determined by flow cytometry as described in "Materials and Methods." The values represent the means ± SD for three separate experiments performed in triplicate. *, significantly greater than values for control; $P \leq 0.05$; **, $P \leq 0.02$. *C*, cells were treated as above for 18 h, after which they were lysed, and the proteins were separated by SDS-PAGE. Proteins were then probed with an antibody directed against phospho(tyrosine-15)-p34^{cdc2}. Each *lane* was loaded with 30 μg of protein. Blots were subsequently stripped and reprobed for actin to ensure equivalent loading and transfer of protein. Alternatively, proteins were immunoprecipitated with an antibody directed against cdc25C and subsequently subjected to Western analysis with an antibody directed against the 14-3-3 protein. Lastly, a 10-μl reaction mixture of cdk1/cdc2 kinase assay was used to separate ^{32}P-labeled histone H1 by 12% SDS-PAGE (*C*, *bottom two panels*). *D*, cells were treated as above for 18 h, after which cdk1/cdc2 activity (expressed as cpm of [γ-^{32}P] incorporated into histone H1) was determined by cdk1/cdc2 kinase assay as described in "Materials and Methods." Values represent the means ± SD for three separate experiments. *, significantly greater than values for UCN-01 alone; $P \leq 0.05$.

particularly 18 h after PD184352/UCN-01 exposure. Consistent with its inhibitory effects on Chk1 (2), UCN-01 modestly reduced the amount of cdc25C phosphatase coimmunoprecipitating with 14-3-3 proteins (Fig. 6*C*). However, this effect was more pronounced in cells treated with both UCN-01 and PD184352. Moreover, cells exposed to the combination of UCN-01 and PD184352 for 18 h exhibited the greatest diminution in phosphorylation of p34^{cdc2} on tyrosine$_{15}$ (Fig. 6*C*). In contrast, total expression of p34^{cdc2} was essentially unchanged. Activity of p34^{cdc2}, reflected by phosphorylation of histone H1, was greater in cells exposed to the combination of UCN-01 and PD184352 than in those exposed to UCN-01 alone at both the 14-h and 18-h intervals (Fig. 6*C*). Lastly, quantification of p34^{cdc2} activity at 18 h by kinase assay confirmed enhanced activation in cells exposed to UCN-01 + PD184352 compared with values obtained for UCN-01 alone (Fig. 6*D*).

Interestingly, caffeine (2 mM; 18 h), an inhibitor of ATM acting upstream of Chk1 (33), also reduced binding of cdc2 to 14-3-3 proteins and, when combined with PD184352, markedly decreased cdc2 phosphorylation. (Fig. 7*A*). Caffeine also substantially increased apoptosis and mitochondrial damage in PD184352-treated cells (Fig. 7*B*). Together, these findings raise the possibility that interactions between PD184352 and UCN-01 may involve interference with checkpoint function and, as a consequence, inappropriate (*i.e.*, unscheduled) activation of p34^{cdc2}.

To identify downstream targets of p42/44 MAPK that might be responsible for or contribute to enhanced apoptosis in UCN-01/PD184352-treated cells, the effects of these agents were examined with respect to expression of p21^{CIP1}, p27^{KIP1}, and CREB, each of which has been linked to antiapoptotic actions (35–37). As shown in Fig. 7*C*, PMA (5 nM; 24 h) robustly increased p21^{CIP1} expression, whereas UCN-01, either alone or in combination with PD184352, had no discernible effect (Fig. 7*C*). Similarly, constitutive expression of p27^{KIP1} in U937 cells was not altered by either drug alone or in combination. However, a clear reduction in expression of phosphorylated CREB was noted in cells exposed to the UCN-01/PD184352 combination. These findings raise the possibility that interference with the downstream MAPK cytoprotective target CREB may contribute to potentiation of apoptosis in UCN-01/PD184352-treated cells.

Studies were also performed in U937 cells stably expressing a p21^{CIP1} antisense construct that are impaired in their capacity to up-regulate p21^{CIP1} in response to PMA (37) and are more sensitive than wild-type cells to apoptosis induced by agents such as 1-β-D-arabinofuranosylcytosine (29). Dysregulation of p21^{CIP1} resulted in a modest but significant increase in apoptosis in cells exposed to UCN-01 or PD184352 individually; moreover, the combination of these agents was significantly more lethal to p21^{CIP1} antisense-expressing cells (Fig. 7*D*). Similar results were observed with PD98059 (data not shown). Because p21^{CIP1} expression is already

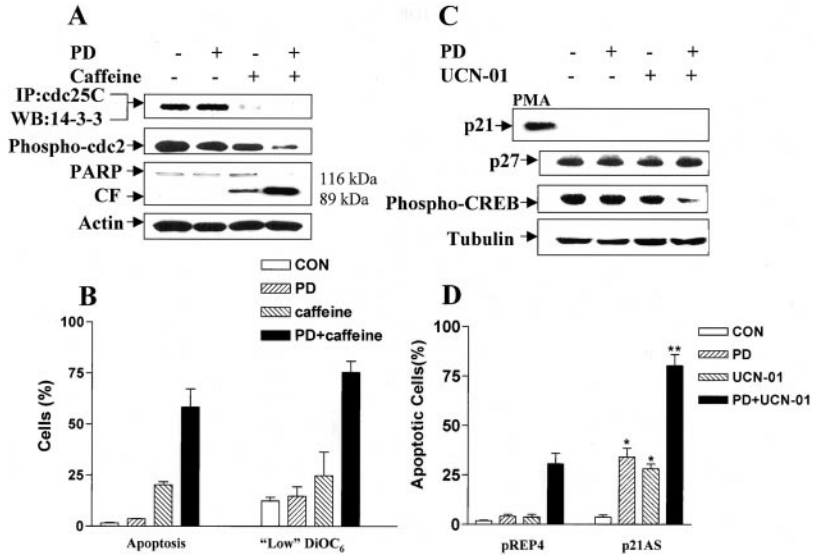

Fig. 7. *A*, cells were treated with PD 184352 (*PD*; 10 μM) ± 2 mM caffeine as above, and the amount of 14-3-3 protein coimmunoprecipitating with cdc25C, phosphorylated p34^{cdc2}, or expression of PARP was determined as described previously. *CF*, cleavage fragment. Each *lane* was loaded with 30 μg of protein. Blots were subsequently stripped and reprobed for actin to ensure equivalent loading and transfer of protein. Two other experiments yielded equivalent results. *B*, cells were treated with PD184352 (*PD*; 10 μM) ± caffeine (2 mM) for 18 h, after which the percentage of apoptotic cells and cells exhibiting a reduction in $\Delta\Psi_m$ determined by morphological assessment or flow cytometry respectively. Values represent the means ± SD for three separate experiments performed in triplicate. *C*, U937 cells were treated with UCN-01 (150 nM) ± PD184352 (*PD*; 10 μM) for 18 h, after which Western analysis was performed to assess expression of p21, p27, and phospho-CREB as described in "Materials and Methods." Each *lane* was loaded with 30 μg of protein. Blots were stripped and reprobed for expression of tubulin to ensure equivalent loading and transfer of protein. Two additional studies yielded comparable results. *D*, U937 cells stably expressing an empty vector (*pREP4*) and a p21^{CIP1} antisense construct (*p21AS*) were exposed to UCN-01 (*UCN*; 150 nM) ± PD 184352 (*PD*; 10 μM) for 18 h, after which the percentage of apoptotic cells was determined by morphological examination as described previously. Values represent the means ± SD for three separate experiments performed in triplicate. *, significantly greater than values for pREP4 cells; $P \leq 0.05$; **, $P \leq 0.02$.

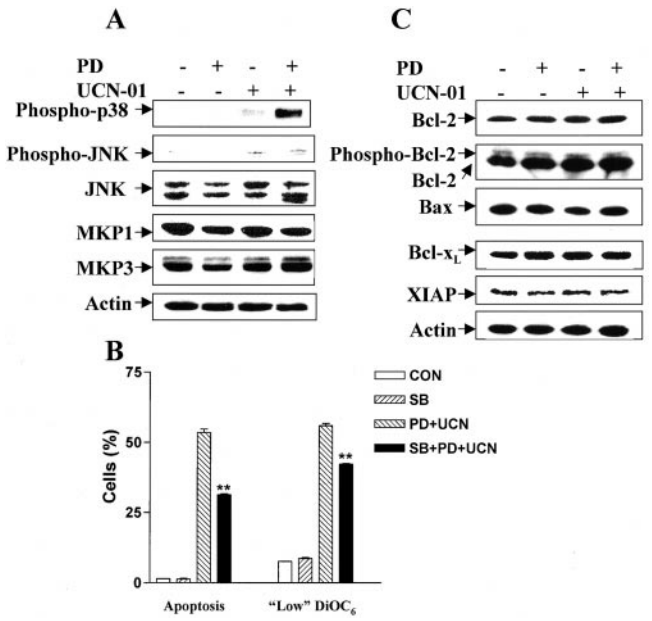

Fig. 8. *A*, U937 cells were exposed to UCN-01 (*UCN*; 150 nM) ± PD184352 (*PD*; 10 μM) for 18 h, after which cells were lysed, and the lysates were separated by SDS-PAGE and probed with antibodies directed against phospho-p38 MAPK, phospho-JNK, total JNK, MKP1, and MKP3. *B*, cells were exposed to PD184352 and UCN-01 as above for 18 h in the presence or absence of the p38 MAPK inhibitor SB203580 (10 μM), after which the percentage of cells exhibiting the morphological features of apoptosis or reduction in $\Delta\Psi_m$, reflected by a diminished uptake of $DiOC_6$, was determined as described previously. Values represent the means ± SD for three separate experiments performed in triplicate. **, significantly less than values for UCN + PD without SB203580; $P \leq 0.02$. *C*, cells were treated as above, after which levels of expression of Bcl-2, Bax, Bcl-x_L, or XIAP were determined by Western analysis as described in "Materials and Methods." Alternatively, proteins were separated by running a 15-cm 12% SDS-PAGE gel, which permitted detection of a putatively phosphorylated, slowly migrating Bcl-2 species (designated phospho-Bcl-2). For *A* and *C*, each *lane* was loaded with 30 μg of protein. Blots were stripped and reprobed for actin to ensure equivalent loading and transfer of protein. In each case, two additional studies yielded comparable results.

dysregulated in the antisense line, these and the preceding findings (Fig. 7*C*) argue against the possibility that potentiation of UCN-01-related apoptosis by MEK/MAPK inhibitors involves impaired induction of the downstream MAPK target $p21^{CIP1}$.

To assess the influence of MEK inhibitors and UCN-01 on other MAPK pathways, the effects of these agents were examined in relation to JNK and p38 phosphorylation (Fig. 8). In contrast to the increase in expression of phospho-MAPK, UCN-01, either alone or in combination with PD184352, did not noticeably induce JNK phosphorylation in U937 cells (Fig. 8*A*). Similar results were obtained with PD98059 (data not shown). In separate studies (38) involving U937 cell transfectants, stable expression of a dominant-negative c-Jun transactivation domain-deficient mutant (TAM67) did not attenuate PD184352/UCN-01-mediated apoptosis (data not shown). Interestingly, coadministration of UCN-01 and PD184352, but not individual drug exposure, resulted in a marked increase in expression of phospho-p38 MAPK. However, coadministration of the p38 MAPK inhibitor SB203580 (10 μM) only partially attenuated apoptosis and mitochondrial injury in PD184352/UCN-01-treated cells (Fig. 8*B*). Lastly, combined drug exposure exerted did not increase expression of the MKP1 and MKP3 phosphatases (Fig. 7*A*). Together, these findings indicate that potentiation of UCN-01-related apoptosis by MEK inhibitors is accompanied by a marked increase in p38 MAPK but not JNK phosphorylation.

To determine whether coadministration UCN-01 and MEK inhibitors modified the expression of apoptotic regulatory proteins, levels of Bcl-2, Bcl-x_L, Bax, and XIAP were monitored by Western analysis (Fig. 8*C*). Coadministration of UCN-01 and PD184352 did not result in a significant change in expression of Bcl-2, Bcl-x_L, Bax, or XIAP. Similar results were observed in cells exposed to the combination of UCN-01 and PD98059 (data not shown). In addition, separation of proteins on a 15-cm, 12% SDS-PAGE gel, which permitted visualization of a slowly migrating, putatively phosphorylated Bcl-2 species (Fig. 7*C*, *second panel from top*), revealed no significant change after exposure of cells to PD184352 in combination with UCN-01. These observations argue against the possibility that potentiation of UCN-01-induced apoptosis by MEK inhibitors stemmed from increased expression of Bax or diminished expression of the antiapoptotic proteins Bcl-2, Bcl-x_L, or XIAP.

Finally, the impact of combined treatment of U937 cells with UCN-01 and PD184352 was examined in relation to effects on clonogenic survival (Fig. 9). UCN-01 (150 nM; 18 h) by itself had a very modest effect on colony formation, whereas PD184352 (10 μM; 18 h) administered alone reduced clonogenic survival by ~40%. However, combined treatment with both agents resulted in a substantial reduction in clonogenicity (*e.g.*, to ~10% of control values; Fig. 9*A*). Furthermore, median dose effect analysis (39) was used to character-

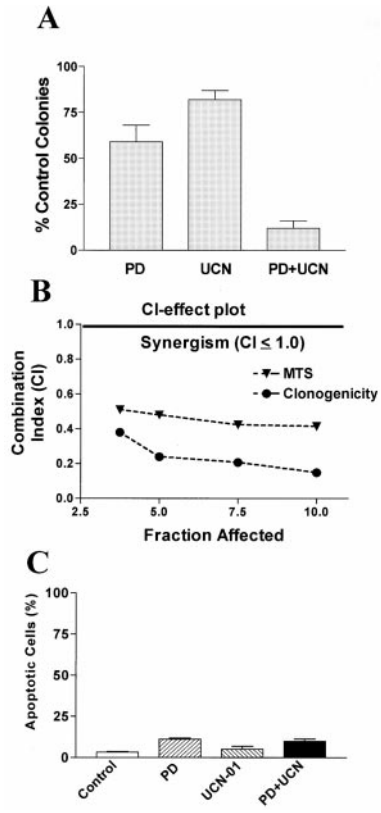

Fig. 9. *A*, cells were exposed to PD184352 (5 μM) ± UCN-01 (100 nM) for 18 h, after which cells were washed free of drug and plated in soft agar as described in the text. After 12 days of incubation, colonies, consisting of groups of ≥50 cells, were scored, and colony formation for each condition was expressed relative to untreated control cells. Values represent the means ± SD for three separate experiments. *B*, U937 cells were exposed to a range of PD184352 (*e.g.*, 3.75–10 μM) and UCN-01 (*e.g.*, 75–200 nM) concentrations alone and in combination at fixed ratio (*e.g.*, 50:1) for 18 h. At the end of this period, colony formation was determined for each condition as above. Alternatively, cell viability was determined using the cell titer 96 reagent as described in "Materials and Methods." In each case, the fraction affected values were determined by comparing results with those of untreated controls, and median dose-effect analysis was used to characterize the nature of the interaction between UCN-01 and PD184352 using a commercially available program (CalcuSyn; Biosoft). ●, values obtained for clonogenic assays; ▼, values obtained for viability assays. Combination index values less than 1.0 denote a synergistic interaction. Two additional studies yielded equivalent results. *C*, normal peripheral blood mononuclear cells were exposed to 150 nM UCN-01 ± 10 μM PD184352 for 18 h, after which the percentage of apoptotic cells was determined by morphological examination as described previously. Values represent the means ± SD for triplicate determination; a second independent study yielded equivalent results.

ize interactions between these agents, administered at a fixed ratio (*e.g.,* PD/UCN-01, 50:1), over a range of UCN-01 concentrations (*e.g.,* 75–200 nM; Fig. 9*B*). Combination index values for the drug combination, using either a reduction in clonogenicity (●) or loss of viability by MTS assay (▼) as end points, were considerably less than 1.0 (Fig. 9*B*), corresponding to a highly synergistic interaction. These findings indicate that enhanced apoptosis in cells exposed to UCN-01 in combination with a MEK/MAPK inhibitor is accompanied by a significant reduction in leukemic cell viability and self-renewal capacity. Finally, parallel studies were carried out using normal peripheral blood mononuclear cells. Exposure of such cells for 24 h to 150 nM UCN-01 ± 10 μM PD184352 did not result in a significant increase in apoptosis for any of the conditions (*e.g.,* <5% increases *versus* controls; $P \geq 0.05$ for each condition). Similar results were observed in cells exposed to the combination of UCN-01 and PD98059 or UO126 (data not shown). These findings raise the possibility that coadministration of UCN-01 with MEK/MAPK inhibitors may not represent a potent apoptotic stimulus in at least some normal hematopoietic cells.

DISCUSSION

The present studies demonstrate that marginally toxic concentrations of the PKC inhibitor and checkpoint abrogator UCN-01 induce activation of the MEK/MAPK pathway in human leukemia cells. Furthermore, interference with this process, *e.g.,* by coadministration of specific MEK inhibitors, potently triggers mitochondrial damage and apoptosis in multiple myeloid and lymphoid leukemia cell types. PKC inhibitors are known to be among the most effective inducers of apoptosis in both hematopoietic and nonhematopoietic cells (40, 41). However, although UCN-01 was originally developed as a specific PKC inhibitor (1), there is evidence that interruption of the PKC pathway, *e.g.,* by UCN-01 (13) or related agents (42), may not be primarily responsible for or sufficient to induce apoptosis in hematopoietic cells. The observations that the PKC inhibitors safingol and GFX failed to interact synergistically with MEK/MAPK inhibitors (Table 1) are in accord with this view and suggest that the antileukemic synergism between UCN-01 and MEK/MAPK inhibitors involves factors other than or in addition to disruption of the PKC pathway.

The finding that structurally dissimilar MEK1/2 inhibitors, which exhibit different mechanisms of action, interact synergistically with UCN-01 to induce apoptosis strongly implicates interference with MAPK activation in the lethality of this drug combination. Whereas PD98059, U0126, and PD184352 oppose Raf-1-induced activation of MEK1/2 (23, 43), U0126 and PD184352 are also potent inhibitors of the MEK1/2 catalytic site (24). However, each of these agents blocked UCN-01-mediated activation of MAPK and promoted mitochondrial damage and cell death. Although MAPK activation has generally been associated with cytoprotective functions (44), it is important to note that disruption of this pathway in U937 cells was not, by itself, a potent inducer of cell death. Such findings are consistent with previous studies demonstrating that interruption of the MAPK cascade by pharmacological or other means potentiates apoptosis in cells exposed to other environmental stresses, *e.g.,* growth factor deprivation (21) or exposure to DNA-damaging agents (27, 45). Collectively, such findings suggest that activation of the MAPK pathway may not be essential for cell survival *per se,* but that it plays a critical role in protecting the cell from a variety of noxious stimuli.

Induction of apoptosis, particularly by chemotherapeutic drugs, has been linked to mitochondrial damage, including loss of the mitochondrial membrane potential or release of pro-apoptotic proteins from the mitochondrial intermembrane space, particularly cytochrome *c* (46). There is some controversy regarding which of these represents the initiating apoptotic event; *e.g.,* the induction of apoptosis in the absence of cytochrome *c* release has been described (47), suggesting a critical role for loss of $\Delta\psi_m$ in cell death decisions. On the other hand, cytochrome *c* release often precedes loss of $\Delta\psi_m$ (48), and a dissociation between apoptotic events and decreases in $\Delta\psi_m$ has been reported in human leukemia cells such as HL-60 and U937 (49). The present findings strongly suggest that cytochrome *c* release represents an upstream event in cells induced to undergo apoptosis by UCN-01 and MEK inhibitors; *e.g.,* whereas the broad caspase inhibitor ZVAD-fmk substantially blocked UCN-01/PD184352-induced apoptosis, caspase activation, and mitochondrial discharge, cytochrome *c* release was unperturbed. Cytochrome *c* release can also be triggered by the Fas/APO-related pathway through activation of procaspase-8 and cleavage/activation of the pro-apoptotic effector, Bid (50). However, the inability of the procaspase-8 inhibitor IETD to oppose apoptosis or cytochrome *c* release argues against a role for the receptor-mediated cell death pathway in the lethal actions of the UCN-01/MEK inhibitor combination.

Recent studies (51) involving malignant lymphoid cells have raised the possibility that kinase inhibitors such as UCN-01 may promote apoptosis by modulating expression of Bcl-2 and related family members or by inducing post-translational modifications (*e.g.,* phosphorylation) in these proteins that interfere with antiapoptotic function. Analogously, PD98059 has been shown to block Bcl-2 phosphorylation and, in so doing, to lower the threshold for growth factor deprivation-induced apoptosis (52). However, we were unable to demonstrate alterations in the expression or in the mobility of Bcl-2 on PAGE electrophoresis, a phenomenon that generally (although not invariably) accompanies perturbations in phosphorylation state (53), nor were changes in levels of expression of several other apoptotic regulatory proteins observed. The complexity of apoptosis regulation is underscored by the numerous events that can modulate this process, including procaspase-9 phosphorylation (54), apaf-1 oligomerization (55), and the release of newly described mitochondrial proteins (*e.g.,* SMAC/Diablo) that antagonize the actions of inhibitors of apoptosis (56). Consequently, the possibility that one or more of these mechanisms operates to enhance apoptosis in leukemic cells exposed to UCN-01 in conjunction with MEK inhibitors cannot be excluded. Studies addressing these issues are currently in progress.

Given the present results, it is tempting to speculate that the lethality of the combination of UCN-01 and MEK inhibitors involves, at least to some extent, interactions at the level of CDK1 ($p34^{cdc2}$). Dysregulation of this CDK (*e.g.,* unscheduled activation) has been identified as a particularly potent inducer of cell death (57) and has been associated with the "mitotic catastrophe," which resembles (although is not identical to) classic apoptosis (58). It is unlikely to be coincidental that the ability of UCN-01, a well-documented inhibitor of Chk1 (2), to induce apoptosis in leukemic cells has been attributed previously (13) to dephosphorylation/activation of CDKs, including $p34^{cdc2}$. It may also be significant that MEK/MAPK activation has been implicated in induction of $p34^{cdc2}$ and cell cycle progression through G_2M (40). Consequently, the notion that cross-talk exists between these pathways appears quite plausible. One possible explanation for the present findings is that the cytoprotective actions of MAPK prevent cells progressing through G_2M from undergoing apoptosis. Conversely, interference with such putative antiapoptotic actions (*e.g.,* by pharmacological MEK/MAPK inhibitors) may permit the pro-apoptotic activity of $p34^{cdc2}$ to proceed unopposed. This concept is supported by the observation that caffeine, which acts upstream of Chk1 at the level of ATM (59), interacted with MEK/MAPK inhibitors in a manner similar to that of UCN-01. Interference with Chk1 activity opposes cdc25C phosphorylation, sequestration by 14-3-3 proteins, and subsequent proteasomal degradation, thereby

allowing this phosphatase to dephosphorylate and activate $p34^{cdc2}$ (3). Thus, in the present studies, coadministration of caffeine, like UCN-01, with PD184352 resulted in reduced binding of the cdc25C phosphatase to 14-3-3 proteins, dephosphorylation of $p34^{cdc2}$, and a marked increase in lethality. Collectively, these findings suggest that the combination of $p34^{cdc2}$ activation with disruption of the MAPK cascade represents a potent apoptotic stimulus, at least in the case of malignant hematopoietic cells.

The possibility that other downstream MAPK effectors contribute to this phenomenon cannot be ruled out, particularly in view of the reduced phosphorylation of CREB noted in UCN-01/PD184352-treated cells. CREB has been identified recently (36, 60) as a cytoprotective target of the Raf→MAPK→Rsk cascade, and it seems plausible that interference with phosphorylation/activation of this transcription factor (*e.g.,* by PD184352) contributed to the observed potentiation of apoptosis. In addition, cross-talk between cytoprotective and stress-related MAPK modules has been described (61), and it is possible that such interactions might contribute to the lethality of the UCN-01/PD184352 combination. In fact, the observations that inhibition of UCN-01-induced MAPK activation by PD184352 was associated with a reciprocal increase in p38 MAPK induction and that coadministration of the p38 MAPK inhibitor SB203580 partially protected cells from apoptosis induced by UCN-01/PD184352 raise the possibility that the p38 MAPK cascade could be involved, at least to some extent, in potentiation of cell death by this drug combination. However, given recent evidence (62) that SB203580 inhibits kinases other than p38 MAPK and the finding that protection from apoptosis by SB203580 was incomplete, it seems highly likely that other factors are involved in the lethal effects of this drug combination. Lastly, the possibility that MEK inhibitors specifically act by interfering with induction of $p21^{CIP1}$, a known MAPK downstream target (63), appears remote, given the findings that: (*a*) UCN-01 failed to induce $p21^{CIP1}$; and (*b*) $p21^{CIP1}$ antisense-expressing cells, which already exhibit dysregulation of this CDKI, displayed enhanced susceptibility to the UCN-01/PD184352 combination. Nevertheless, these findings remain compatible with a cytoprotective role for basal $p21^{CIP1}$ expression, a phenomenon that has been described previously (64).

In summary, the present studies demonstrate that the kinase inhibitor and checkpoint antagonist UCN-01 unexpectedly activates MAPK in human leukemia cells and that interference with this process by multiple pharmacological MEK/MAPK inhibitors leads to a marked potentiation of mitochondrial injury (*e.g.,* cytochrome *c* release), caspase activation, and apoptosis. Moreover, these events occur in a variety of myeloid and lymphoid leukemia cell types, indicating that this phenomenon is not lineage-specific. Finally, enhanced apoptosis in these cells is associated with perturbations in several signaling and cell cycle regulatory pathways, including dephosphorylation of $p34^{cdc2}$ and CREB, as well as activation of p38 MAPK. Significantly, such observations raise the possibility that interruption of multiple signaling pathways (*e.g.,* by pharmacological kinase inhibitors) may provide a particularly potent apoptotic stimulus, at least in malignant hematopoietic cells. Aside from providing insights into factors that regulate the lethal actions of UCN-01, these findings have potential therapeutic implications; *e.g.,* in humans, levels of free UCN-01 achievable in the plasma and potentially available to tumor cells are limited by extensive binding of this agent to α_1 acidic glycoprotein (14). It is conceivable that MEK inhibitors, particularly those which, like PD184352, are active *in vivo* (26), could potentiate the antileukemic activity of pharmacologically relevant concentrations of UCN-01. In this regard, it would be of interest to determine whether synergistic interactions between UCN-01 and MEK/MAPK inhibitors could be extended to other hematological and nonhematological tumor types. Accordingly, studies addressing this question are currently underway.

REFERENCES

1. Mizuno, K., Noda, K., Ueda, Y., Hanaki, H., Saido, T. C., Ikuta, T., Kuroki, T., Tamaoki, T., Hirai, S., and Osada, S. UCN-01, an anti-tumor drug, is a selective inhibitor of the conventional PKC subfamily. FEBS Lett., *359:* 259–261, 1995.
2. Graves, P. R., Yu, L., Schwarz, J. K., Gales, J., Sausville, E. A., O'Connor, P. M., and Piwnica-Worms, H. The Chk1 protein kinase and the Cdc25C regulatory pathways are targets of the anticancer agent UCN-01. J. Biol. Chem., *275:* 5600–5605, 2000.
3. Peng, C-Y., Gravesa, P. R., Thoma, R. S., Wu, Z., Shaw, A. S., and Piwnica-Worms, H. Mitotic and G_2 checkpoint control: regulation of 14-3-3 protein binding by phosphorylation of Cdc25C on serine-216. Science (Wash. DC), *277:* 1501–1505, 1997.
4. Bunch, R. T., and Eastman, A. Enhancement of *cis*-platinum-induced cytotoxicity by 7-hydroxystaurosporine, a new G_2 checkpoint inhibitor. Clin. Cancer Res., *2:* 791–797, 1996.
5. Akinaga, S., Nomura, K., Gomi, K., and Okabe, M. Enhancement of antitumor activity of mitomycin C *in vitro* and *in vivo* by UCN-01, a selective inhibitor of protein kinase C. Cancer Chemother. Pharmacol., *32:* 183–189, 1993.
6. Shao, R-G., Cao, C-X., Shimizu, T., O'Connor, P. M., Kohn, K. W., and Pommier, Y. Abrogation of an S-phase checkpoint and potentiation of camptothecin cytotoxicity by 7-hydroxystaurosporine (UCN-01) in human cancer cell lines, possibly influenced by p53 function. Cancer Res., *57:* 4029–4035, 1997.
7. Harvey, S., Decker, R., Dai, Y., Schaefer, G., Tang, L., Kramer, L., Dent, P., and Grant, S. Interactions between 2-fluoroadenine 9-β-D-arabinofuranoside and the kinase inhibitor UCN-01 in human leukemia and lymphoma cells. Clin. Cancer Res., *7:* 320–330, 2001.
8. Shi, Z., Azuma, A., Sampath, D., Li, Y. X., Huang, P., and Plunkett, W. S-Phase arrest by nucleoside analogues and abrogation of survival without cell cycle progression by 7-hydroxystaurosporine. Cancer Res., *61:* 1065–1072, 2001.
9. Tang, L., Boise, L. H., Dent, P., and Grant, S. Potentiation of 1-β-D-arabinofuranosylcytosine-mediated mitochondrial damage and apoptosis in human leukemia cells (U937) overexpressing bcl-2 by the kinase inhibitor 7-hydroxystaurosporine (UCN-01). Biochem. Pharmacol., *60:* 1445–1456, 2000.
10. Wang, S., Vrana, J. A., Bartimole, T. M., Freemerman, A. J., Jarvis, W. D., Kramer, L. B., Krystal, G., Dent, P., and Grant, S. Agents that down-regulate or inhibit protein kinase C circumvent resistance to 1-β-D-arabinofuranosylcytosine-induced apoptosis in human leukemia cells that overexpress Bcl-2. Mol. Pharmacol., *52:* 1000–1009, 1997.
11. Akinaga, S., Nomura, K., Gomi, K., and Okabe, M. Effect of UCN-01, a selective inhibitor of protein kinase C, on the cell-cycle distribution of human epidermoid carcinoma, A431 cells. Cancer Chemother. Pharmacol., *33:* 273–280, 1994.
12. Chen, X., Lowe, M., and Keyomarsi, K. UCN-01-mediated G_1 arrest in normal but not tumor breast cells is pRb-dependent and p53-independent. Oncogene, *18:* 5691–5702, 1999.
13. Wang, Q., Worland, P. J., Clark, J. L., Carlson, B. A., and Sausville, E. A. Apoptosis in 7-hydroxystaurosporine-treated T lymphoblasts correlates with activation of cyclin-dependent kinases 1 and 2. Cell Growth Differ., *6:* 927–936, 1995.
14. Fuse, E., Tanii, H., Takai, K., Asanome, K., Kurata, N., Kobayashi, H., Kuwabara, T., Kobayashi, S., and Sugiyama, Y. Altered pharmacokinetics of a novel anticancer drug, UCN-01, caused by specific high affinity binding to α1-acid glycoprotein in humans. Cancer Res., *59:* 1054–1060, 1999.
15. Kurata, N., Kuwabara, T., Tanii, H., Fuse, E., Akiyama, T., Akinaga, S., Kobayashi, H., Ymaguchi, K., and Kobayashi, S. Pharmacokinetics and pharmacodynamics of a novel protein kinase inhibitor UCN-01. Cancer Chemother. Pharmacol., *44:* 12–18, 1999.
16. Wilson, W. H., Sorbara, L., Figg, W. D., Mont, E. K., Sausville, E., Warren, K. E., Balis, F. M., Bauer, K., Raffeld, M., Senderowicz, A. M., and Monks, A. Modulation of clinical drug resistance in a B-cell lymphoma patient by the protein kinase inhibitor 7-hydroxystaurosporine: presentation of a novel therapeutic paradigm. Clin. Cancer Res., *6:* 415–421, 2000.
17. Leppa, S., and Bohmann, D. Diverse functions of JNK signaling and c-Jun in stress response and apoptosis. Oncogene, *18:* 6158–6162, 1999.
18. Verheij, M., Bose, R., Lin, X. H., Yao, B., Jarvis, W. D., Grant, S., Birrer, M. J., Szabo, E., Zon, L. I., Kyriakis, J. M., Haimovitz-Friedman, A., Fuks, Z., and Kolesnick, R. Requirement for ceramide-initiated SAPK/JNK signaling in stress-induced apoptosis. Nature (Lond.), *380:* 75–79, 1996.
19. Segar, R., and Krebs, E. G. The MAPK signaling cascade. FASEB J., *9:* 726–735, 1995.
20. Cross, T. G., Scheel-Toellner, D., Henriquez, N. V., Deacon, E., Salmon, M., and Lord, J. M. Serine/threonine protein kinases and apoptosis. Exp. Cell Res., *256:* 34–41, 2000.
21. Xia, Z., Dickens, M., Raingeaud, J., Davis, R., and Greenberg, M. E. Opposing effects of ERK and JNK-p38 MAP kinases on apoptosis. Science (Wash. DC), *270:* 1326–1331, 1995.
22. Tibbles, L. A., and Woodgett, J. R. The stress-activated protein kinase pathways. Cell. Mol. Life Sci., *55:* 1230–1254, 1999.
23. Dudley, D. T., Pang, L., Decker, S. J., Bridges, A. J., and Saltiel, A. R. A synthetic inhibitor of the mitogen-activated protein kinase cascade. Proc. Natl. Acad. Sci. USA, *92:* 7686–7689, 1995.
24. Favata, M. F., Horiuchi, K. Y., Manos, E. J., Daulerio, A. J., Stradley, D. A., Feeser, W. S., Van Dyk, D. E., Pitts, W. J., Earl, R. A., Hobbs, F., Copeland, R. A., Magolda,

R. L., Scherle, P. A., and Trzaskos, J. M. Identification of a novel inhibitor of mitogen-activated protein kinase kinase. J. Biol. Chem., *273:* 18623–18632, 1998.
25. Davis, S., Vanhoutte, P., Pages, C., Caboche, J., and Laroche, S. The MAPK/ERK cascade targets both Elk-1 and cAMP response element-binding protein to control long-term potentiation-dependent gene expression in the dentate gyrus *in vivo*. J. Neurosci., *20:* 4563–4572, 2000.
26. Sebolt-Leopold, J. S., Dudley, D. T., Herrera, R., Van Becelaere, K., Wiland, A., Gowan, R. C., Tecle, H., Barrett, S. D., Bridges, A., Przybranowski, S., Leopold, W. R., and Saltiel, A. R. Blockade of the MAP kinase pathway suppresses growth of colon tumors *in vivo*. Nat. Med., *5:* 810–816, 1999.
27. Jarvis, W. D., Fornari, F. A., Jr., Tombes, R. M., Erukulla, R. K., Bittman, R., Schwartz, G. K., Dent, P., and Grant, S. Evidence for involvement of mitogen-activated protein kinase, rather than stress-activated protein kinase, in potentiation of 1-β-D-arabinofuranosylcytosine-induced apoptosis by interruption of protein kinase C signaling. Mol. Pharmacol., *54:* 844–856, 1998.
28. Vrana, J. A., and Grant, S. Synergistic induction of apoptosis in human leukemia cells (U937) exposed to bryostatin 1 and the proteasome inhibitor lactacystin involves dysregulation of the PKC/MAPK cascade. Blood, *97:* 2107–2114, 2001.
29. Wang, Z., Van Tuyle, G., Conrad, D., Fisher, P. B., Dent, P., and Grant, S. Dysregulation of the cyclin-dependent kinase inhibitor p21WAF1/CIP1/MDA6 increases the susceptibility of human leukemia cells (U937) to 1-β-D-arabinofuranosylcytosine-mediated mitochondrial dysfunction and apoptosis. Cancer Res., *59:* 1259–1267, 1999.
30. Gorczyca, W., Gong, J., and Darzynkiewicz, Z. Detection of DNA strand breaks in individual apoptotic cells by the *in situ* terminal deoxynucleotidyl transferase and nick translation assays. Cancer Res., *53:* 1945–1951, 1993.
31. Jarvis, W. D., Povirk, L. F., Turner, A. J., Traylor, R. S., Gewirtz, D. A., Pettit, G. R., and Grant, S. Effects of bryostatin 1 and other pharmacological activators of protein kinase C on 1-[β-D-arabinofuranosyl]cytosine-induced apoptosis in HL-60 human promyelocytic leukemia cells. Biochem. Pharmacol., *47:* 839–852, 1994.
32. Peng, C. Y., Graves, P. R., Ogg, S., Thoma, R. S., Byrnes, M. J., Wu, Z., Stephenson, M. T., and Piwnica-Worms, H. C-TAK1 protein kinase phosphorylates human Cdc25C on serine 216 and promotes 1-3-3 binding. Cell Growth Differ., *9:* 197–208, 1998.
33. Blasina, A., Price, B. D., Turenne, G. A., and McGowan, C. H. Caffeine inhibits the checkpoint kinase ATM. Curr. Biol., *9:* 1135–1138, 1999.
34. Suzuki, A., Tsutomi, Y., Yamamoto, N., Shibutani, T., and Akahane, K. Mitochondrial regulation of cell death: mitochondria are essential for procaspase 3-p21 complex formation to resist Fas-mediated cell death. Mol. Cell. Biol., *19:* 3842–3847, 1999.
35. St. Croix, B., Florenes, V. A., Rak, J. W., Flanagan, M., Bhattacharya, N., Slingerland, J. M., and Kerbel, R. S. Impact of the cyclin-dependent kinase inhibitor p27Kip1 on resistance of tumor cells to anticancer agents. Nat. Med., *2:* 1204–1210, 1996.
36. Bonni, A., Brunet, A., West, A. E., Datta, S. R., Takasu, M. A., and Greenberg, M. E. Cell survival promoted by the Ras-MAPK signaling pathway by transcription-dependent and -independent mechanisms. Science (Wash. DC), *286:* 1358–1362, 1999.
37. Wang, Z., Su, Z. Z., Fisher, P. B., Wang, S., VanTuyle, G., and Grant, S. Evidence of a functional role for the cyclin-dependent kinase inhibitor p21(WAF1/CIP1/MDA6) in the reciprocal regulation of PKC activator-induced apoptosis and differentiation in human myelomonocytic leukemia cells. Exp. Cell Res., *244:* 105–116, 1998.
38. Freemerman, A. J., Turner, A. J., Birrer, M. J., Szabo, E., Valerie, K., and Grant, S. Role of c-jun in human myeloid leukemia cell apoptosis induced by pharmacological inhibitors of protein kinase C. Mol. Pharmacol., *49:* 788–795, 1996.
39. Chou, T-C., and Talalay, P. Quantitative analysis of dose-effect relationships: the combined effects of multiple drugs or enzyme inhibitors. Adv. Enzyme Regul., *22:* 27–55, 1984.
40. Bertrand, R., Solary, E., O'Connor, P., Kohn, K. W., and Pommier, Y. Induction of a common pathway of apoptosis by staurosporine. Exp. Cell Res., *211:* 314–321, 1994.
41. Jarvis, W. D., Turner, A. J., Povirk, L. F., Traylor, R. S., and Grant, S. Induction of apoptotic DNA fragmentation and cell death in HL-60 human promyelocytic leukemia cells by pharmacological inhibitors of protein kinase C. Cancer Res., *54:* 1707–1714, 1994.
42. Harkin, S. T., Cohen, G. M., and Gescher, A. Modulation of apoptosis in rat thymocytes by analogs of staurosporine: lack of direct association with inhibition of protein kinase C. Mol. Pharmacol., *54:* 663–670, 1998.
43. Davies, S. P., Reddy, H., Caivano, M., and Cohen, P. Specificity and mechanism of action of some commonly used protein kinase inhibitors. Biochem. J., *351:* 95–105, 2000.
44. Tsuneoka, M., and Mekada, E. Ras/MEK signaling suppresses Myc-dependent apoptosis in cells transformed by c-myc and activated ras. Oncogene, *19:* 115–123, 2000.
45. Persons, D. L., Yazlovitskaya, E. M., and Pelling, J. C. Effect of extracellular signal-regulated kinase on p53 accumulation in response to cisplatin. J. Biol. Chem., *275:* 35778–35785, 2000.
46. Yang, J., Liu, X., Bhalla, K., Kim, C. N., Ibrado, A. M., Cai, J., Peng, T. I., Jones, D. P., and Wang, X. Prevention of apoptosis by Bcl-2: release of cytochrome c from mitochondria blocked. Science (Wash. DC), *275:* 1129–1132, 1997.
47. Chauhan, D., Pandey, P., Ogata, A., Teoh, G., Krett, N., Halgren, R., Rosen, S., Kufe, D., Kharbanda, S., and Anderson, K. Cytochrome c-dependent and -independent induction of apoptosis in multiple myeloma cells. J. Biol. Chem., *272:* 29995–29997, 1997.
48. Bossy-Wetzel, E., Newmeyer, D. D., and Green, D. R. Mitochondrial cytochrome c release in apoptosis occurs upstream of DEVD-specific caspase activation and independently of mitochondrial transmembrane depolarization. EMBO J., *17:* 37–49, 1998.
49. Finucane, D. M., Waterhouse, N. J., Amarante-Mendes, G. P., Cotter, T. G., and Green, D. R. Collapse of the inner mitochondrial transmembrane potential is not required for apoptosis of HL60 cells. Exp. Cell Res., *251:* 166–174, 1999.
50. Sun, X. M., MacFarlane, M., Zhuang, J., Wolf, B. B., Green, D. R., and Cohen, G. M. Distinct caspase cascades are initiated in receptor-mediated and chemical-induced apoptosis. J. Biol. Chem., *274:* 5053–5060, 1999.
51. Kitada, S., Zapata, J. M., Andreeff, M., and Reed, J. C. Protein kinase inhibitors flavopiridol and 7-hydroxy-staurosporine down-regulate antiapoptosis proteins in B-cell chronic lymphocytic leukemia. Blood, *96:* 393–397, 2000.
52. Deng, X., Ruvolo, P., Carr, B., and May, W. S., Jr. Survival function of ERK1/2 as IL-3-activated, staurosporine-resistant Bcl2 kinases. Proc. Natl. Acad. Sci. USA, *97:* 1578–1583, 2000.
53. Haldar, S., Jena, N., and Croce, C. M. Inactivation of Bcl-2 by phosphorylation. Proc. Natl. Acad. Sci. USA, *92:* 4507–4511, 1995.
54. Cardone, M. H., Roy, N., Stennicke, H. R., Salvesen, G. S., Franke, T. F., Stanbridge, E., Frisch, S., and Reed, J. C. Regulation of cell death protease caspase-9 by phosphorylation. Science (Wash. DC), *282:* 1318–1321, 1998.
55. Cain, K., Bratton, S. B., Langlais, C., Walker, G., Brown, D. G., Sun, X. M., and Cohen, G. M. Apaf-1 oligomerizes into biologically active approximately 700-kDa and inactive approximately 1.4-MDa apoptosome complexes. J. Biol. Chem., *275:* 6067–6070, 2000.
56. Chai, J., Du, C., Wu, J. W., Kyin, S., Wang, X., and Shi, Y. Structural and biochemical basis of apoptotic activation by Smac/DIABLO. Nature (Lond.), *406:* 855–862, 2000.
57. Shimizu, T., O'Connor, P. M., Kohn, K. W., and Pommier, Y. Unscheduled activation of cyclin B1/Cdc2 kinase in human promyelocytic leukemia cell line HL60 cells undergoing apoptosis induced by DNA damage. Cancer Res., *55:* 228–231, 1995.
58. King, K. L., and Cidlowski, J. A. Cell cycle and apoptosis: common pathways to life and death. J. Cell. Biochem., *58:* 175–180, 1995.
59. Zhou, B. B., Chaturvedi, P., Spring, K., Scott, S. P., Johanson, R. A., Mishra, R., Mattern, M. R., Winkler, J. D., and Khanna, K. K. Caffeine abolishes the mammalian G(2)/M DNA damage checkpoint by inhibiting ataxia-telangiectasia-mutated kinase activity. J. Biol. Chem., *275:* 10342–10348, 2000.
60. Riccio, A., Ahn, S., Davenport, C. M., Blendy, J. A., and Ginty, D. D. Mediation by a CREB family transcription factor of NGF-dependent survival of sympathetic neurons. Science (Wash. DC), *286:* 2358–2361, 1999.
61. Ganiatsas, S., Kwee, L., Fujiwara, Y., Perkins, A., Ikeda, T., Labow, M. A., and Zon, L. I. SEK1 deficiency reveals mitogen-activated protein kinase cascade crossregulation and leads to abnormal hepatogenesis. Proc. Natl. Acad. Sci. USA, *95:* 6881–6886, 1998.
62. Lali, F. V., Hunt, A. E., Turner, S. J., and Foxwell, B. M. The pyridinyl imidazole inhibitor SB203580 blocks phosphoinositide-dependent protein kinase activity, protein kinase B phosphorylation, and retinoblastoma hyperphosphorylation in interleukin-2-stimulated T cells independently of p38 mitogen-activated protein kinase. J. Biol. Chem., *275:* 7395–7402, 2000.
63. Pumiglia, K. M., and Decker, S. J. Cell cycle arrest mediated by the MEK/mitogen-activated protein kinase pathway. Proc. Natl. Acad. Sci. USA, *94:* 448–452, 1997.
64. Park, J-S., Carter, S., Reardon, D. B., Schmidt-Ullrich, R., Dent, P., and Fisher, P. B. Roles for basal and stimulated $p21^{Cip\text{-}1/WAF1/MDA6}$ expression and mitogen-activated kinase signaling in radiation-induced cell cycle checkpoint control in carcinoma cells. Mol. Biol. Cell, *10:* 4231–4246, 1999.